

High signal-to-noise ratio differential conductance spectroscopy

Hamed Alemansour,¹ S. O. Reza Moheimani,^{1, a)} James H. G. Owen,² John N. Randall,² and Ehud Fuchs²

¹⁾Erik Jonsson School of Engineering and Computer Science, The University of Texas at Dallas, Richardson, TX 75080, USA

²⁾Zyvec Labs LLC, 1301 N Plano Rd., Richardson, TX 75081, USA

The scanning tunneling microscope (STM) has enabled manipulation and interrogation of surfaces with atomic-scale resolution. Electronic information about a surface is obtained by combining the imaging capability of the STM with scanning tunneling spectroscopy (STS), i.e. measurement of current-voltage (I/V) characteristics of the surface. We propose a change in the STM feedback loop that enables capturing a higher quality dI/dV image. A high frequency dither voltage is added to the bias voltage of the sample and the fundamental frequency component of the resulting current is demodulated. The in-phase component of this signal is then plotted along with the X and Y position data, constructing the dI/dV image. We show that by incorporating notch filters in the STM feedback loop, we may utilize a high-amplitude dither voltage to significantly improve the quality of the obtained dI/dV image.

I. INTRODUCTION

The invention of the scanning tunneling microscope in the early 1980s by Binnig & Rohrer was a major breakthrough in the field of microscopy¹. STM relies on the concept of quantum tunneling. A sharp tip is brought within subnanometer distance of a conductive surface. By applying a bias voltage between the sample and the tip, electrons tunnel through the vacuum separating the two. In constant current mode, a feedback control system keeps the tunneling current constant by varying the tip-sample separation. Here, the topographic image can be constructed using the controller output along with the X and Y position data.

Since the invention of STM, there have been ongoing efforts to improve the already existing spectroscopic modes and to develop new techniques to unravel important electronic properties of the surface. A number of spectroscopy modes have been developed and are available today, including inelastic electron tunneling spectroscopy (IETS)²⁻⁴, time-resolved scanning tunneling microscopy (TRSTM)^{5,6}, as well as I-V⁷⁻⁹ and I-Z^{10,11} spectroscopy modes. Current-Voltage spectroscopy, also known as scanning tunneling spectroscopy (STS), is perhaps the most widely used spectroscopic mode of STM, which provides information about electronic properties of the surface. In particular, $d(\ln I)/d(\ln V)$ is a good measure of the local density of states (LDOS) of the surface.

An STS spectrum can be obtained by positioning the STM tip above a particular location, freezing the tip Z position, and measuring the tunneling current as a function of the bias voltage. Then, the slope of the I-V curve at each bias voltage, dI/dV, corresponds to the sample's local electron density of states (LDOS). In addition, the dI/dV signal can provide information about the spatial variation of electronic wave functions, and single-electron tunneling (SET) phenomena¹². This is a slow process that could be affected by the piezoelectric actuator's drift, which changes the XY position and tip-sample height and thus the measured current. An alternative is to acquire a scanning tunneling spectroscopy spectrum by means of a modulation technique. Compared to the numerical

derivation of an I-V curve, measuring dI/dV by the lock-in technique enhances the signal-to-noise ratio (SNR). Using the lock-in technique, a dI/dV image at the bias voltage V can be obtained simultaneously with the topography image without the need for disabling the feedback loop. However, images that are obtained from this method suffer from noise, which is mainly due to the small amplitude of the dither voltage. The signal level must be kept small to avoid perturbing the feedback loop as a high amplitude dither voltage is fed back to the controller and disturbs the topography image. Here, we report a method that enables increasing the SNR of dI/dV imaging using the lock-in technique. We show that with a small change in the feedback loop, we can improve the quality of differential conductance imaging by utilizing a large amplitude dither voltage, without introducing noise into the STM image.

II. METHODS

A home built Lyding-style ultra high vacuum STM¹³, operating at room temperature, is used to perform the experiments described here. The base pressure of the STM is as low as 10^{-11} Torr. A ZyVector¹⁴ STM control system is used to handle real-time control tasks with a sampling frequency of 100 kHz.

The experiments were performed on H-terminated Si(100) samples. To prepare a sample, a piece of 1 ohm cm boron-doped wafer is degassed at 650° C for 8 hours. The surface oxide film and any carbon contamination are removed by flashing the sample three times to 1250° C for 30 s. Then, the sample is cooled to 350° C and is exposed to a flux of atomic H for 4 min. This is generated by a 1300° C tungsten filament cracking the background H₂ molecules into atomic H¹⁵.

The tunneling current between the tip and the sample can be expressed as¹⁶:

$$I = \frac{4\pi e}{\hbar} \int_0^{eV} \rho_{tip}(\epsilon - eV) \rho_{sample}(\epsilon) T(\epsilon, V, d) d\epsilon \quad (1)$$

with ρ_{tip} , ρ_{sample} , and $T(\epsilon, V, d)$ representing the density of states of the tip, density of states of the sample, and the transmission factor for tunneling from a tip to a sample state. If the particle energy is much smaller than the vacuum level, then

^{a)}Corresponding author: Reza.Moheimani@utdallas.edu

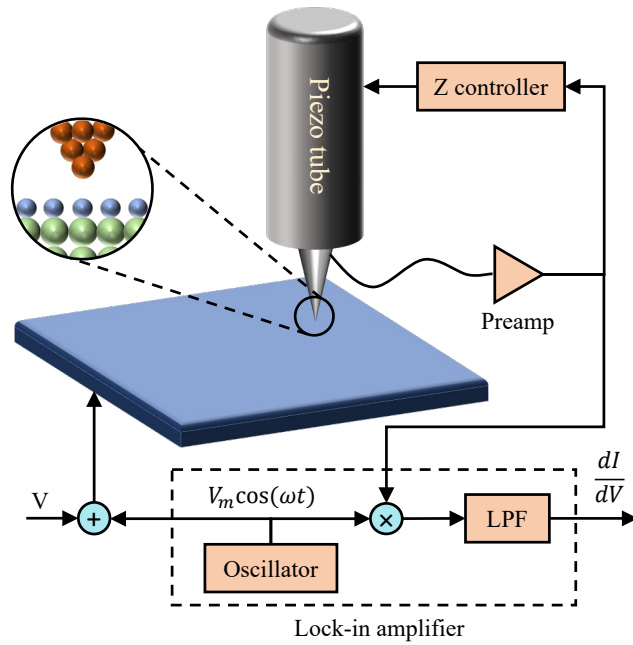


FIG. 1. The block diagram of STM for the measurement of dI/dV .

the transmission coefficient can be expressed as^{16,17}:

$$T \propto \exp(-\text{const.} \cdot d \sqrt{\phi}) \quad (2)$$

with d and ϕ being the barrier thickness and the barrier height, respectively.

For STS, the tunnel current is proportional to the density of available states from the Fermi level up to the bias voltage. Therefore, the current-to-voltage characteristics of the tunneling junction is utilized to measure the local density of states (LDOS). The differential conductance dI/dV is obtained by taking the first derivative of the tunneling current in Eq. 1 with respect to V as follows:

$$\frac{dI}{dV} = \frac{4\pi e^2}{\hbar} \rho_{\text{tip}}(0) \rho_{\text{sample}}(eV) T(eV, V, d) \quad (3)$$

Therefore, assuming that the density of states of the metal tip and the transmission factor are voltage independent, then the differential conductance is proportional to the density of states of the sample¹⁶.

To obtain differential conductance at a bias voltage of V , a dither voltage $V_m \cos(\omega t)$ is added to the sample bias voltage. For a low frequency dither signal, it can be assumed that the measured current is primarily due to the quantum tunneling with the capacitive current being negligible. Therefore, to obtain differential conductance for specified points within a pre-defined voltage range, the bias voltage is slowly swept during the measurements and for each point dI/dV is recorded.

The I-V curve can be represented by a function f as $I = f(V + V_m \cos(\omega t))$. Using the Taylor series expansion of I around the voltage V , it can be shown that the amplitude of signal at $n\omega$ is proportional to the n th derivative of I with respect to V . For a low frequency dither signal, the quadrature

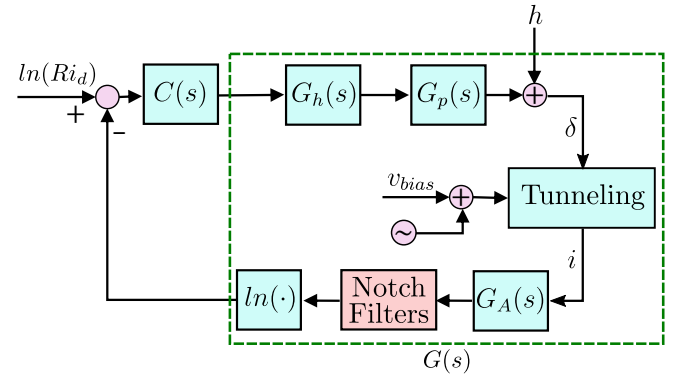


FIG. 2. The modified STM feedback loop. $C(s)$, $G_h(s)$, and $G_p(s)$ are controller, high voltage amplifier, and Z axis actuator, respectively. $G_A(s)$ is the preamplifier with an amplification gain of k .

component is negligible and the amplitude of the signal at ω is equal to dI/dV . On the other hand, the quadrature component would be substantial for a high frequency dither signal and it should be taken into account. In this case, the amplitude of the in-phase component of the current at the fundamental frequency represents dI/dV and the quadrature part is proportional to the capacitance. In practice, the amplitude of fundamental frequency can be obtained by a lock-in amplifier, as shown in Fig. 1. A dither voltage $V_m \cos(\omega t)$ is generated by the lock-in amplifier and added to the sample bias voltage V . The resulting current is then sent back to the lock-in amplifier and is compared with the reference signal to be demodulated to the in-phase and quadrature components.

In order to increase the amplitude of the dither voltage and obtain high quality differential capacitance images, we added five notch filters to the feedback loop of the STM as shown in Fig. 2. With these filters in the feedback path, a higher amplitude dither signal can be used to obtain the dI/dV image without any adverse effect on the topography image. This change in the feedback loop of STM can greatly enhance the quality of STS.

III. RESULTS AND DISCUSSION

We performed a series of experiments on a H-terminated Si(100) surface to investigate the effect of incorporating notch filters in the feedback loop on the signal-to-noise ratio of STS. In these experiments, the bias voltage of the sample and the set-point current were set to -2.5 V and 1 nA, respectively. A Zurich Instruments HF2LI 50 MHz lock-in amplifier was used to generate a 700 Hz dither signal, which was added to the bias voltage and applied to the sample. We used a FEMTO LCA-400K-10M transimpedance amplifier with the bandwidth of 400 kHz and the amplification gain of 10^7 as the preamplifier. The amplified current was sent to a ZyVector¹⁴ box, which is used for control and image processing purposes. It was also sent back to the lock-in amplifier and separated into in-phase and quadrature components at the fundamental frequency. The in-phase component of the signal was sent to

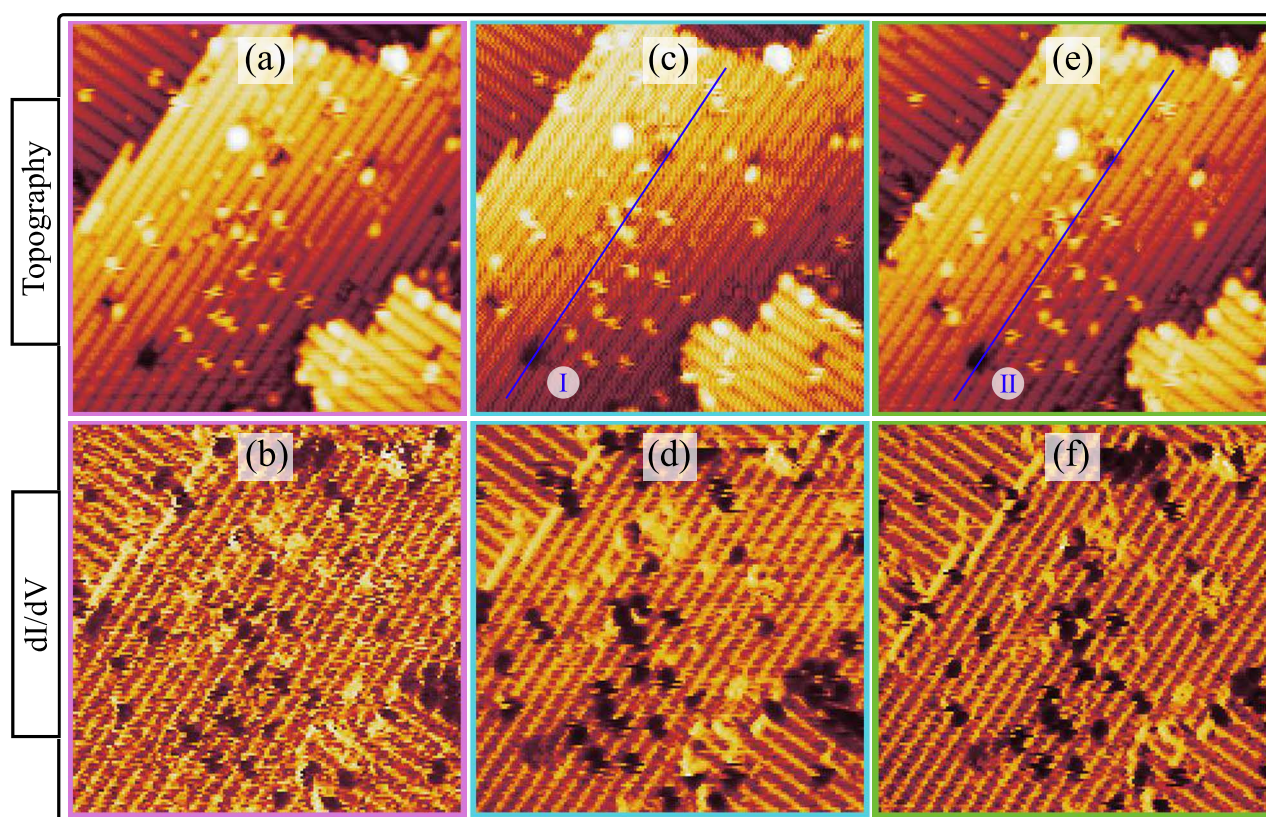


FIG. 3. The topography image (top row) and dI/dV image (bottom row) of a Si(100)-2 \times 1:H passivated surface. (a)-(b) without notch filters and with a small amplitude dither voltage ($V_m = 0.1$ V), (c)-(d) without notch filters and with a large amplitude dither voltage ($V_m = 0.5$ V), and (e)-(f) with notch filters and with a large amplitude dither voltage ($V_m = 0.5$ V).

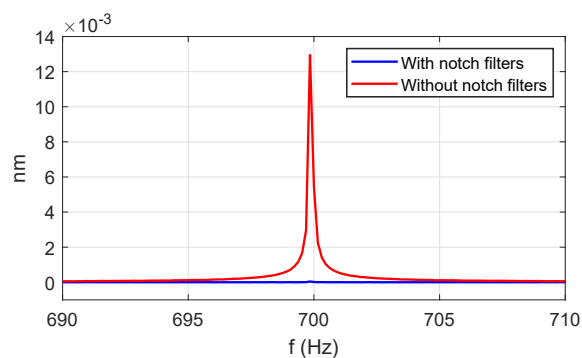


FIG. 4. Single-sided amplitude spectrum of topography with and without notch filters in the feedback loop.

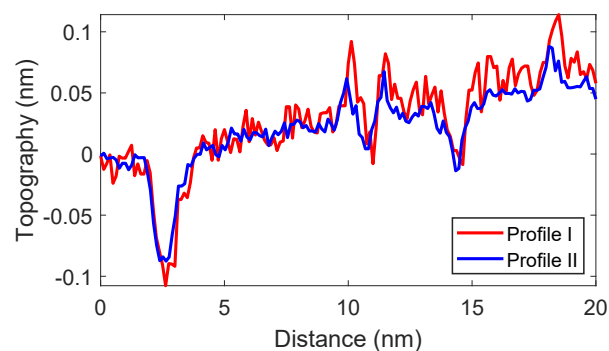


FIG. 5. Comparison of profiles I and II in Fig. 3. The SNR is enhanced by using notch filters in the feedback loop.

ZyVector¹⁴ and used for producing dI/dV images in real time.

A typical topography image and its corresponding dI/dV image for a dither amplitude of 0.1 V are shown in Fig. 3(a) and 3(b), respectively. Fig. 3(b) shows that the obtained dI/dV is quite noisy and has a low SNR. By increasing the dither voltage to 0.5 V, the SNR of differential conductance image is improved as shown in Fig. 3(d). However, although the dither signal is out of the bandwidth of the control system, nonetheless it finds its way into the controller and disturbs the

feedback loop operation. This makes the topography image in the Fig. 3(c) noisy. For a high amplitude dither, these perturbations in the tip-sample height may cause a tip-sample crash. This can change the tip rendering both the tip and the sample unusable.

To obtain high quality images for both the topography and the dI/dV , we incorporated five notch filters at 1 kHz, 2 kHz, 3 kHz, 4 kHz, and 5 kHz into the feedback loop. The 3 dB

bandwidth of all the filters was 0.2 kHz. These filters attenuate the current signal at the fundamental frequency of the dither voltage and its first few harmonics. This enhances the SNR of the topography image and simultaneously increases the quality of dI/dV , as shown in Fig. 3(e) and Fig. 3(f), respectively. Fig. 4 compares the single-sided amplitude spectrum of topography with and without notch filters in the feedback loop. This demonstrates the SNR improvement that may be achieved with this method. For dither voltages more than 0.5 V, the standard deviation of noise exceeds 0.1 Å. This is comparable to topographic features on the sample and results in noticeable noise on the topography image. To visualize the noise content of topography image more clearly, two profiles are drawn along a same dimer row and are shown with blue lines on Fig. 3. We observe in Fig. 5 that the topography profile II in Fig. 3(e) is much smoother than its counterpart in Fig. 3(c).

We use a Zurich Instruments lock-in amplifier to measure the amplitude of the component of current which is in-phase with the dither voltage. This small current is corrupted by measurement noise appearing at the lock-in amplifier output. Since this is then utilized by our digital control system, ZyVector¹⁴, to construct a dI/dV image, this measurement noise has an adverse impact on the resolution of the image. The dI/dV image in Fig. 3(f) clearly demonstrates the higher resolution of our method in comparison with the conventional method, shown in Fig. 3(b). To quantify this, we recorded the dI/dV signal at the output of the lock-in amplifier with a sampling rate of 28.78 kHz over a 20 s time period. The lateral position of the STM tip was kept constant during this experiment. The SNR, defined as the ratio of the mean to the standard deviation of dI/dV , was measured as 1.145 with the conventional dI/dV method. It was increased to 3.953 with our method. This 24.78 dB enhancement in SNR was made possible by incorporating notch filters in the feedback loop that enabled us to increase the dither amplitude from $V_m = 0.1$ V to $V_m = 0.5$ V.

IV. CONCLUSIONS

Scanning tunneling microscopy has a wide range of applications in science and technology. In this work, we introduced a small, but powerful, change in the feedback control system of the STM, which greatly improves the SNR of scanning tunneling spectroscopy. Implementation of this method does not require additional hardware and all the required modules can be added to the control software package of most STMs. We showed that by filtering the dither frequency and its higher harmonics from the feedback loop, the amplitude of the dither voltage can be increased in STS leading to higher quality dI/dV images. The effectiveness of this method was experimentally examined. Having demonstrated proof-of-principle of this spectroscopy method, we have confirmed the reproducibility of the improved SNR of dI/dV images, by performing similar experiments with several different samples and tips. Furthermore, by allowing us to maintain the feedback control loop during the collection of the dI/dV data, we

maintain the tip-sample distance, and thus obtain more reliable data.

ACKNOWLEDGMENTS

This material is based upon work supported by the U.S. Department of Energy's Office of Energy Efficiency and Renewable Energy (EERE) under the Advanced Manufacturing Office Award No. DE-EE0008322.

This report was prepared as an account of work sponsored by an agency of the United States Government. Neither the United States Government nor any agency thereof, nor any of their employees, makes any warranty, express or implied, or assumes any legal liability or responsibility for the accuracy, completeness, or usefulness of any information, apparatus, product, or process disclosed, or represents that its use would not infringe privately owned rights. Reference herein to any specific commercial product, process, or service by trade name, trademark, manufacturer, or otherwise does not necessarily constitute or imply its endorsement, recommendation, or favoring by the United States Government or any agency thereof. The views and opinions of authors expressed herein do not necessarily state or reflect those of the United States Government or any agency thereof.

DATA AVAILABILITY

The data that support the findings of this study are available within the article.

- ¹G. Binnig, H. Rohrer, Ch. Gerber, and E. Weibel. Surface Studies by Scanning Tunneling Microscopy. *Physical Review Letters*, 49(1):57–61, 1982.
- ²G. Binnig, N. Garcia, and H. Rohrer. Conductivity sensitivity of inelastic scanning tunneling microscopy. *Physical Review B*, 32(2):1336–1338, 1985.
- ³J. Lambe and R. C. Jaklevic. Molecular Vibration Spectra by Inelastic Electron Tunneling. *Physical Review*, 165(3):821–832, January 1968.
- ⁴A. S. Hallbäck, N. Oncel, J. Huskens, H. J. Zandvliet, and B. Poelsema. Inelastic Electron Tunneling Spectroscopy on Decanethiol at Elevated Temperatures. *Nano Letters*, 4(12):2393–2395, December 2004.
- ⁵B. S. Swartzentruber, A. P. Smith, and H. Jónsson. Experimental and Theoretical Study of the Rotation of Si Ad-dimers on the Si(100) Surface. *Physical Review Letters*, 77(12):2518–2521, September 1996.
- ⁶R. J. Hamers. Ultrafast time resolution in scanned probe microscopies: Surface photovoltage on Si(111)-(7×7). *Journal of Vacuum Science & Technology B: Microelectronics and Nanometer Structures*, 9(2):514, March 1991.
- ⁷J. A. Stroscio, R. M. Feenstra, and A. P. Fein. Electronic Structure of the Si(111)2×1 Surface by Scanning-Tunneling Microscopy. *Physical Review Letters*, 57(20):2579–2582, November 1986.
- ⁸M. F. Crommie, C. P. Lutz, and D. M. Eigler. Confinement of Electrons to Quantum Coralls on a Metal Surface. *Science*, 262(5131):218–220, 1993.
- ⁹N. Nilius. Development of One-Dimensional Band Structure in Artificial Gold Chains. *Science*, 297(5588):1853–1856, August 2002.
- ¹⁰F. Tajaddodianfar, S. O. R. Moheimani, and J. N. Randall. Scanning Tunneling Microscope Control: A Self-Tuning PI Controller Based on Online Local Barrier Height Estimation. *IEEE Transactions on Control Systems Technology*, 27(5):2004–2015, September 2019.
- ¹¹F. Tajaddodianfar, S. O. R. Moheimani, J. Owen, and J. N. Randall. On the effect of local barrier height in scanning tunneling microscopy: Measurement methods and control implications. *Review of Scientific Instruments*, 89(1):013701, January 2018.

This is the author's peer reviewed, accepted manuscript. However, the online version of record will be different from this version once it has been copyedited and typeset.

PLEASE CITE THIS ARTICLE AS DOI: 10.1116/6.0000823

- ¹²H. J. Zandvliet and A. van Houselt. Scanning Tunneling Spectroscopy. *Annual Review of Analytical Chemistry*, 2(1):37–55, July 2009.
- ¹³S. H. Tessmer, D. J. Van Harlingen, and J. W. Lyding. Integrated cryogenic scanning tunneling microscopy and sample preparation system. *Review of Scientific Instruments*, 65(9):2855–2859, 1994.
- ¹⁴<https://www.zyvexlabs.com/apm/products/zyvector/>. [Online; accessed 23-November-2020].

- ¹⁵S. O. R. Moheimani and H. Alemansour. A new approach to removing H atoms in hydrogen depassivation lithography. In Eric M. Panning and Martha I. Sanchez, editors, *Novel Patterning Technologies for Semiconductors, MEMS/NEMS and MOEMS 2020*. SPIE, March 2020.
- ¹⁶B. Voigtländer. *Scanning Probe Microscopy*. Springer Berlin Heidelberg, 2015.
- ¹⁷H. Alemansour, S. O. R. Moheimani, J. H. G. Owen, J. N. Randall, and E. Fuchs. Controlled removal of hydrogen atoms from H-terminated silicon surfaces. *Journal of Vacuum Science & Technology B*, 38(4):040601, July 2020.